

Atmospheric behaviour of particulate oxalate at UK urban background and rural sites



Bunthoon Laongsri^a, Roy M. Harrison^{a,b,*}

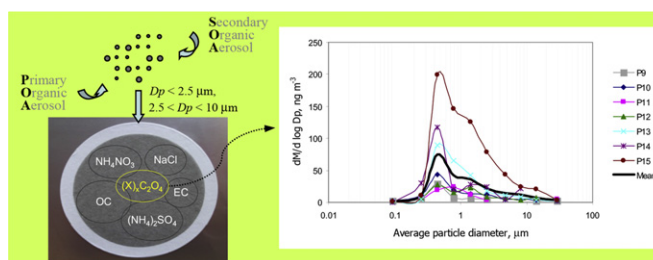
^aDivision of Environmental Health & Risk Management, School of Geography, Earth & Environmental Sciences, University of Birmingham, Edgbaston, Birmingham B15 2TT, United Kingdom

^bDepartment of Environmental Sciences/Center of Excellence in Environmental Studies, King Abdulaziz University, PO Box 80203, Jeddah 21589, Saudi Arabia

HIGHLIGHTS

- ▶ Oxalate was measured at urban and rural sites.
- ▶ Inter-site and intra-site correlations indicate a predominantly secondary source.
- ▶ Emissions from traffic and biomass combustion are small.
- ▶ Trajectory clustering demonstrates advection from mainland Europe.
- ▶ Particle size distribution is similar to sulphate.

GRAPHICAL ABSTRACT



ARTICLE INFO

Article history:

Received 14 August 2012

Received in revised form

1 February 2013

Accepted 7 February 2013

Keywords:

Oxalate

Secondary organic aerosol

Regional pollution

ABSTRACT

Oxalic acid is widely reported in the literature as one of the major components of organic aerosol. It has been reported as both a product of primary emissions from combustion processes and as a secondary product of atmospheric chemistry. Concentrations of particulate oxalate have been measured at a UK urban site (500 daily samples) and for a more limited period simultaneously at a rural site (100 samples) in the fine (less than 2.5 μm) and coarse (2.5–10 μm) size fractions. Full size distributions have also been measured by sampling with a MOUDI cascade impactor. Average concentrations of oxalate sampled over different intervals in PM₁₀ are 0.04 ± 0.03 μg m⁻³ at the rural site and 0.06 ± 0.05 μg m⁻³ at the urban background site, broadly comparable with measurements from other European locations. During the period of simultaneous sampling at the urban and rural site, concentrations were very similar and the inter-site correlation in the PM_{2.5} fraction for oxalate ($r = 0.45$; $p < 0.001$) was appreciably weaker than that for sulphate and nitrate ($r = 0.82$ and 0.84 , respectively). Nonetheless, the data clearly point to a predominantly secondary source of oxalate at these sites. Possible contributions from road traffic and woodsmoke appear to be very small. In the larger urban dataset, oxalate in PM_{2.5} was correlated significantly ($p < 0.01$) with sulphate ($r = 0.60$), nitrate ($r = 0.48$) and secondary organic carbon ($r = 0.25$). Clustering of air mass back trajectories demonstrates the importance of advection from mainland Europe. The size distribution of oxalate at the urban site showed a major mode at around 0.55 μm and a minor mode at around 1.5 μm in the mass distribution. The former mode is similar to that for sulphate suggesting either a similar in-cloud formation mechanism, or cloud processing of oxalate and sulphate after formation in homogeneous reaction processes.

© 2013 Elsevier Ltd. All rights reserved.

* Corresponding author. Division of Environmental Health & Risk Management, School of Geography, Earth & Environmental Sciences, University of Birmingham, Edgbaston, Birmingham B15 2TT, United Kingdom. Tel.: +44 121 414 3494; fax: +44 121 414 3708.

E-mail address: r.m.harrison@bham.ac.uk (R.M. Harrison).

1. Introduction

Organic compounds, including both water-soluble and insoluble species, account for a significant fraction of the fine particulate matter mass in the atmosphere (Jacobson et al., 2000; Zhang et al., 2007; Harrison and Yin, 2008). Among the different types of water-soluble organic carbon (WSOC), monocarboxylic acids (MCA) and dicarboxylic acids (DCA) are groups of significant interest in the chemical characterisation of PM (Chebbi and Carlier, 1996; Cecinato et al., 1999; Dabek-Zlotorzynska and McGrath, 2000; Limbeck et al., 2001; Falkovich et al., 2004; Karthikeyan and Balasubramanian, 2005; Wang et al., 2007).

Oxalic acid is the dominant dicarboxylic acid (DCA) followed by malonic and succinic acids (Kawamura and Ikushima, 1993; Kawamura and Usukura, 1993; Yao et al., 2002a,b), and it constitutes up to 50–70% of total atmospheric DCA (Sempere and Kawamura, 1994, 1996). The occurrence of oxalate in aerosols and precipitation was demonstrated using ion chromatography by Norton et al. (1983). Thereafter, Kawamura and Kaplan (1987) found that the diacids (C_2 – C_{10}) were mainly associated with particles but a minor fraction of these compounds was present in the vapour phase. They suggested the possibility that low molecular weight diacids (i.e. oxalic) were present in the vapour phase under elevated temperature conditions. Oxalic acid is mostly present in the particulate phase in the ambient atmosphere and is of lower volatility compared with formic and acetic acids, which are the main monocarboxylic acids present in the gas phase (Chebbi and Carlier, 1996).

The sources of oxalate in the atmosphere comprise both primary biogenic and anthropogenic emissions (Kawamura and Kaplan, 1987; Kawamura and Ikushima, 1993) and transformations of precursors in the gaseous and condensed phases (Dabek-Zlotorzynska and McGrath, 2000; Chebbi and Carlier, 1996; Kawamura et al., 1996; Myriokefalitakis et al., 2011). Knowledge of the size distribution of oxalate can provide valuable insights into its sources, formation and growth mechanism. Oxalate is predominantly found in size distributions in the large droplet mode, while the condensation mode and the coarse mode are both relatively less abundant (Kerminen et al., 2000; Yao et al., 2003; Huang et al., 2006).

In this paper, we aim to gain a better understanding of the sources and atmospheric behaviour of particulate oxalate by analysis of a dataset of oxalate concentrations from two UK sites in comparison with other, major chemical components i.e. sulphate, nitrate, chloride, primary and secondary organic carbon (OC) and elemental carbon (EC) in ambient air.

2. Methodology

2.1. Sampling locations

2.1.1. Elms Road Observatory Site (EROS) (N 52:27:13; W 1:55:41)

EROS is located within the “green space” of the University of Birmingham campus. This is an urban background site located in an open field within the University. The site is about 3.5 km southwest of the centre of Birmingham, which has a population of over one million and is part of a conurbation of 2.5 million population. The nearest anthropogenic sources are a nearby railway (predominantly electric), some moderately trafficked B roads at about 500 m and other activities of the university and local residents. Fig. S1 in Supplementary Information shows the locations of the two sites.

2.1.2. Harwell (N 51:34:16; W 1:19:31)

This rural site is located within the grounds of the Harwell Science Centre, Didcot, Oxfordshire. The air sampler was installed

outside the main monitoring station. The surrounding area is generally open with agricultural fields. There is limited activity in the area and the nearest road about 400 m from the monitoring site is used only for access to buildings within the Science Park. The nearest trees are at a distance of 200–300 m from the monitoring station. Distant sources include the busy A34 dual carriageway about 2 km to the east and the Didcot Power Station about 5 km to the north-east. The Harwell site is located 115 km from the EROS site, both in central England.

2.2. Air sampling

Airborne particulate matter in both fine ($PM_{2.5}$) and coarse ($PM_{2.5-10}$) fractions was collected daily by Partisol samplers with filter changing taking place at 1200 noon local time over the period from November 2008 to April 2011 at EROS and from July to December 2010 at Harwell. A Dichotomous Partisol Plus model 2025D sequential air sampler fitted with a PM_{10} inlet and containing a virtual impactor and downstream flow controllers which separate the flow into fine and coarse fractions, at flow rates of 15.0 L min^{-1} and 1.7 L min^{-1} , respectively was utilised. The calculation of coarse PM is achieved by the correction of fine particles in the carrier flow using the formula, $C_c = M_c/V_t - V_c/V_f \cdot C_f$ (where C_c is the mass concentration of the coarse particle fraction, M_c the mass collection on coarse particle fraction filter, V_c and V_t are the volumes of air samples through the coarse fraction filters and the sum of coarse and fine fraction filters, respectively, and C_f is mass concentration of the fine particle fraction). The Partisol sampler was equipped with a 47 mm quartz fibre filter (Whatman QMA) substrate. Filters were pre-heated at 500°C in air using a furnace for 4 h in order to minimize their carbon content and stored sealed in a freezer prior to air sampling. The exposed filters were stored in filter cassettes within the storage magazines inside of the instrument. After the sampling was completed, the exposed filters were stored in a metal container at about -18°C in a freezer until analysis to prevent loss of volatile compounds. This sampling method is subject to the usual artefacts of adsorption and volatilisation which occur when sampling semi-volatile materials on filters.

Samples were also collected at the EROS site using a MOUDI cascade impactor run at 30 L min^{-1} , giving cut points at 10, 5.6, 3.2, 1.8, 1.0, 0.56, 0.32 and $0.18 \mu\text{m}$. Impaction substrates were 47 mm Teflon with a 37 mm Teflon back-up. Because of its reduced pressure the MOUDI is liable to under-sample semi-volatile particulate substances including nitrate (Huang et al., 2004) and oxalate.

2.3. Analysis of samples

2.3.1. OC, EC and TC

For the determination of OC, EC and TC concentration, a Sunset Laboratory Thermal-Optical Carbon Aerosol Analyser was used in this study. It uses thermal desorption in combination with optical transmission of laser light through the sample to speciate carbon collected on a quartz fibre filter (Sunset Laboratory Inc., 2004). Organic carbon is removed during an initial non-oxidizing temperature ramp from about 75°C to 650°C under a helium atmosphere, and then passes to a manganese dioxide oxidizing oven where it is converted to carbon dioxide, which is mixed with hydrogen and converted to methane over a heated nickel catalyst. The methane is subsequently measured using a flame ionization detector (FID). A second temperature ramp from 500°C to 850°C is then initialized with the carrier gas switched to a helium/oxygen mixture, under which elemental carbon and pyrolysis products are oxidized and carried through the system and measured in the same manner as the organic carbon. A laser is used to monitor the light

transmission through the filter during the analysis, which determines a split point which separates the elemental carbon formed by charring during the initial non-oxidising temperature ramp from the elemental carbon that was originally in the sample. The split point is the point in time when the laser signal measured during the oxidizing stage equals the initial laser signal. The temperature programme used a protocol recently developed for the European Super-sites for Atmospheric Aerosol Research project (EUSAAR 2), which is He at 200 °C (120 s); 300 °C (150 s); 450 °C (180 s); 650 °C (180 s) following by He/O₂ 500 °C (120 s); 550 °C (120 s); 700 °C (70 s) and 850 °C (80 s) (Cavalli et al., 2010). A filter punch 1.5 cm² in size was removed from the 47-mm QMA filter and loaded into the carbon aerosol analyser. The results of OC/EC analysis were corrected for the blank.

Organic carbon concentrations were sub-divided into primary and secondary OC using the elemental carbon tracer method (Castro et al., 1999), as reinterpreted by Pio et al. (2011). This involved estimating primary OC as equal to 0.35 EC and secondary OC by difference from the total.

2.3.2. Ionic species

The exposed QMA filters remaining from carbon analysis and PTFE filters were transferred from their bags to a narrow neck 15 mL HDPE bottle. Distilled deionised water (10 mL) was added and the bottles were extracted in an ultrasonic bath for 30 min at room temperature. After ultrasonication, the filter extracts were filtered through a syringe filter (0.2 µm) and then kept in a cold room until analysis. For particulate matter collected onto PTFE filters in size-segregated samples, the filters were wetted with propan-2-ol (0.5 mL) to eliminate the natural hydrophobicity of the filters. Then, 15 mL of ddw were added and ultrasonication performed for 30 min. The leachate was filtered and kept refrigerated until being analysed.

Anion concentrations (sulphate, nitrate, chloride and oxalate) were determined using ion chromatography (Dionex model ICS-2000). The ICS-2000 is an integrated ion chromatography system containing an analytical column (IonPac AS11HC with 2 × 250 mm) with a guard column (IonPac AG11HC with 2 × 50 mm). The eluent for these samples was potassium hydroxide (gradient) and its flow rate during the analyses was 0.38 mL min⁻¹. The injection sample volume of 200 µL was loaded into the eluent stream and 5 mL sample vials were used with the auto sampler. The ICS-2000 was

controlled by Chromeleon software which also provided data acquisition and data processing functions. The IC system was calibrated using a series of mixed anion standards of known concentration (0.2–20 ppm) before running a sample. The mixed standard solutions containing SO₄²⁻, NO₃⁻, Cl⁻ and C₂O₄²⁻ were prepared and kept in the cold room.

2.3.3. Quality assurance

The quality of chemical analysis was investigated and detailed in the [Supplementary Information](#). After completion of the work, it was learned that oxalate is susceptible to degradation in aqueous solutions (Dabek-Zlotorzynska and McGrath, 2000). As our samples had been stored for periods between 2 and 28 days as aqueous extracts at 4 °C prior to analysis, statistical tests were applied to evaluate oxalate losses. Application of the Mann–Whitney test showed no significant difference between samples stored for 7 days and 25 days, and for < 7 days and >7 days, and we conclude that degradation losses were negligible.

2.4. Air mass trajectories calculation

In order to investigate the potential source regions of oxalate, backward air mass trajectories were calculated for the period of study. The Hybrid Single Particle Lagrangian Integrated Trajectory (HYSPPLIT_4) model available on the NOAA Laboratory website was used for calculation of the trajectories. The meteorological data used (the Global Data Assimilation System; GDAS) were obtained at the NOAA Air Resource Laboratory (ARL) archives. Each of the trajectories corresponded to a 72 h back trajectory ending at 500 m altitude at each site. A cluster analysis was applied to minimise the uncertainty of individual trajectories associated with the resolution and accuracy of the meteorological data and by any simplifying assumptions used in the trajectory model (Stohl, 1998).

3. Results and discussion

3.1. Oxalate concentration level and major chemical composition in PM

Table 1 shows the concentrations of oxalate in PM in comparison with published data from other sites from Europe and Asia. The differences in oxalate concentration depend on the local sources as

Table 1
Average concentrations (µg m⁻³) of oxalic acid in airborne particulate matter in some previous studies.

Site	Period	Size fraction	Oxalic acid concentration	References
Urban background ^a , UK	Nov 08–Apr 11	PM _{2.5}	0.05 ± 0.05	This work
		PM _{2.5–10}	0.02 ± 0.01	
		PM ₁₀	0.06 ± 0.05	
Rural, UK ^a	Jul–Dec 10	PM _{2.5}	0.02 ± 0.03	This work
		PM _{2.5–10}	0.02 ± 0.01	
		PM ₁₀	0.04 ± 0.03	
		–	0.052 ± 0.029	
Mountain, Austria	Apr 99	–	0.068 ± 0.023	Limbeck et al., 2005
Urban background, Austria	Feb 99	–	0.019	Cecinato et al., 1999
Urban, Italy	1997	PM ₁₀	0.008	
Semi-rural, Italy	1994	PM ₁₀	0.007	Rohrl and Lammel, 2001
Forest, Italy	1994	PM ₁₀	0.021–0.432	
Coastal rural, Germany	Feb–Mar 98	TSP	0.004–0.157	
Rural, Germany	Nov–Dec 99; Jul–Aug 98	TSP	0.064–0.497	
Urban, Germany	Jul–Aug 98	TSP	0.050 ± 0.37	Saarnio et al., 2010
Urban, Finland ^a	Apr–May 06;	PM _{2.5}	0.140 ± 0.024	
Urban background, Romania	Jul–Sep 06	PM ₁	0.035 ± 0.023	Arsene et al., 2011
		PM _{1.5}	0.049 ± 0.032	
Urban, China	Jan 07 – Mar 08	PM _{>1.5}	0.182 ± 0.106	Ho et al., 2011
	Dec 06–Jan 08	PM _{2.5}	0.216 ± 0.097	
	July–Aug 07	PM _{2.5}	0.114 ± 0.696	
Urban, India	Jan 07 – May 07	PM ₁₀		Pavuluri et al., 2010

^a Reported as concentration of oxalate.

well as on the variability in meteorological and atmospheric chemical conditions in the area at the time of sampling. In our dataset, oxalate exhibited higher concentrations in fine particulate matter than in the coarse fraction especially for aerosol samples taken at the urban site.

The major anion components of the aerosol samples were also measured in order to investigate relationships of oxalate with those constituents, and their concentration data appear in Table S1 in the Supplementary Information.

3.1.1. Effect of the local factors upon oxalate concentration

Regression analysis of ionic species in PM_{2.5} obtained from simultaneously collected EROS and Harwell samples was conducted using reduced major axis (RMA) regression. The relationships of concentrations of oxalate and other chemical components between the two sites are summarized in Table 2. In these data, the correlation coefficients (*r*) of sulphate and nitrate in fine particles show quite high values of 0.82 and 0.84, respectively. On the other hand, lower values of correlation coefficient for chloride, oxalate, WSOC and OC_{sec} between the sites were observed in the range from 0.45 to 0.57.

The plot for sulphate in the fine mode showed a zero intercept with a gradient close to 1.0, indicating that the regional contribution of long-range transport in the atmosphere plays a dominant role in determining its concentration. For nitrate in PM_{2.5}, the regression intercept in Table 2 indicates a small local increment of 0.11 μg m⁻³ consistent with the local fine nitrate contribution of 0.17 μg m⁻³ estimated from the difference in mean concentrations of data from simultaneously collected samples from the two sites (Table 3). This finding suggests a small nitrate urban increment, as was concluded for London by Abdalmogith and Harrison (2005), although the observation of a similar increment of SO₄²⁻ at EROS indicates that it may simply reflect slightly greater regional formation at EROS. With regard to chloride, oxalate and WSOC, the intercept values in the fine fraction were low (0.05 μg m⁻³, 0.01 μg m⁻³ and 0.01 μg m⁻³, respectively) suggesting regional sources and no significant urban effect. The Mann–Whitney *U* test was applied to assess whether any significant concentration difference for aerosol components existed between the two sites. This test is a nonparametric test that can be used to analyse data from two independent groups. Test results indicated that SO₄²⁻, NO₃⁻, C₂O₄²⁻ and OC_{sec} concentrations measured in PM_{2.5} simultaneously at EROS and Harwell were not significantly different, with *p* > 0.05. There were differences for Cl⁻, EC, OC_{prim}, OC and WSOC concentrations in fine particles between the two sites (*p* < 0.05). The estimation of an urban contribution to atmospheric aerosol was quantified by subtraction of Harwell concentrations representing the rural site from EROS concentrations representing an urban background site. The results for the local contribution can be

inferred from Table 3. As expected, EC shows a strong local contribution (0.6 μg m⁻³) in PM_{2.5} reflecting local urban emissions at the EROS site. OC_{sec} and OC_{prim} in fine particles show a lower local contribution (0.4 μg m⁻³ and 0.3 μg m⁻³). Small local contributions were observed in fine sulphate, nitrate and chloride in this study (0.13 μg m⁻³, 0.17 μg m⁻³ and 0.08 μg m⁻³, respectively). There is no difference in mean concentrations of oxalate in PM_{2.5} between the two sites although concentrations are low and less precise than for the other analytes. This finding is strongly supportive of the formation of oxalate by regional-scale atmospheric chemical processes and atmospheric transport and its presence as a long-lived species. Backward air mass trajectories arriving at both sites are reported in a subsequent section in order to investigate further the origins of the regional contribution.

3.2. Seasonal variation of oxalate

The time series of oxalate measured daily in the fine fraction at the EROS and Harwell sites is shown in Fig. 1. It is clear that the within-site temporal variation of oxalate was greater than the spatial variation. In order to evaluate seasonal variations, monthly concentration data for major components are presented in Fig. 2. The air sampling period was split into four seasons as follows: summer (JJA); autumn (SON); winter (DJF) and spring (MAM). The significance of differences in ionic concentrations between the seasons was determined for EROS data by applying a Kruskal–Wallis test. The number of data in the whole, summer, autumn, winter and spring periods were 500, 116, 165, 101 and 118 samples, respectively. In these data, test results indicated significant differences for each of sulphate, nitrate, chloride and oxalate concentrations between the four seasons (*p* < 0.05). It is clear that sulphate, nitrate and chloride in the fine fraction were lower in the summer months (Fig. 2), but the dataset is too small to draw firm conclusions. For chloride, the mean concentration in PM_{2.5} and PM₁₀ is higher in the winter and lower in the summer as expected due to generally much higher wind speeds in winter leading to greater generation of marine aerosol. A seasonal trend for particulate oxalate does not show through so clearly but the average concentration level is highest in spring. This may be the result of strong sunshine levels and plant growth favouring secondary formation, with lower temperatures than in summer reducing the partitioning into vapour. Kerminen et al. (2000) saw a clear summer maximum and winter minimum at sites in Finland.

3.3. Sources and formation pathways of oxalate by correlation analysis

An intra-site correlation analysis of measured components at EROS was conducted in order to investigate the origin of particles (Table S3). Oxalate in PM_{2.5} and PM₁₀ shows a slightly higher correlation (*r* value) with sulphate (*r* = 0.60 and *r* = 0.59, respectively) than with nitrate (*r* = 0.48 and *r* = 0.49, respectively) for the entire period. These results suggest that oxalate originates from similar atmospheric processes as sulphate i.e., from secondary formation. The close relationship of oxalate with sulphate is consistent with results reported by Kerminen et al. (2000), Yao et al. (2003) and Yu et al. (2005). Strong relationships of oxalate with sulphate and nitrate are observed particularly in summer (for PM_{2.5}, *r* = 0.70 and *r* = 0.79, respectively; for PM₁₀, *r* = 0.69 and *r* = 0.78, respectively). The correlations between oxalate and nitrate suggest that temperature may influence the oxalate concentration as it does for nitrate through the ammonium nitrate dissociation. This has recently been confirmed in field observations by Bao et al. (2012), although laboratory studies of the atmospheric gas-particle

Table 2
Results of regression analyses of EROS (urban background) and Harwell (rural) concentrations of ionic components in PM_{2.5}.

Analyte	RMA regression ^a
Sulphate	$y = 1.09x$ ($r = 0.82$)
Nitrate	$y = 1.05x + 0.11$ ($r = 0.84$)
Chloride	$y = 1.13x + 0.05$ ($r = 0.52$)
Oxalate	$y = 0.67x + 0.01$ ($r = 0.45$)
WSOC	$y = 1.25x + 0.01$ ($r = 0.52$)
OC _{sec} ^b	$y = 1.62x - 0.67$ ($r = 0.57$)

^a *y* represents urban background (EROS) concentration of analyte in μg m⁻³; *x* represents rural (Harwell) concentration of analyte in μg m⁻³.

^b Secondary organic carbon calculated based on the ratio of (OC/EC)_{min} = 0.35.

Table 3Statistical data on the concentrations ($\mu\text{g m}^{-3}$) at EROS and Harwell sites during the simultaneous period ($n = 100$).

	PM _{2.5}		PM _{2.5–10}		PM ₁₀	
	Mean	Range	Mean	Range	Mean	Range
EROS						
SO ₄ ²⁻	1.60 ± 1.35	0.32–6.48	0.25 ± 0.17	<dl–0.89	1.85 ± 1.47	0.55–7.37
NO ₃ ⁻	1.61 ± 2.11	<dl–10.88	0.63 ± 0.64	<dl–3.29	2.25 ± 2.50	<dl–12.49
Cl ⁻	0.35 ± 0.27	<dl–1.29	0.61 ± 0.51	0.08–2.79	0.96 ± 0.67	0.16–3.38
C ₂ O ₄ ²⁻	0.02 ± 0.02	<dl–0.10	0.01 ± 0.01	<dl–0.05	0.03 ± 0.02	<dl–0.12
EC	1.0 ± 1.1	0.2–8.2	0.04 ± 0.1	<dl–0.5	1.0 ± 1.1	0.2–8.3
OC	2.3 ± 1.6	0.9–12.1	1.2 ± 0.6	0.5–5.3	3.5 ± 1.8	1.6–13.7
OC _{prim}	0.4 ± 0.4	0.1–2.9	n.a	n.a	0.4 ± 0.4	0.1–2.9
OC _{sec} ^a	2.0 ± 1.3	0.7–9.2	n.a	n.a	3.1 ± 1.5	1.4–10.8
WSOC	1.7 ± 1.0	0.1–6.7	n.a	n.a	n.a	n.a
WSOC/OC _{sec}	0.9 ± 0.2	0.1–1.2	n.a	n.a	n.a	n.a
HAR						
SO ₄ ²⁻	1.47 ± 1.24	0.05–6.76	0.35 ± 0.40	<dl–2.36	1.82 ± 1.40	0.36–7.53
NO ₃ ⁻	1.44 ± 2.02	0.03–11.65	0.71 ± 0.68	<dl–3.40	2.16 ± 2.50	0.19–14.75
Cl ⁻	0.27 ± 0.23	<dl–1.22	0.66 ± 0.60	0.04–3.17	0.93 ± 0.80	0.09–4.39
C ₂ O ₄ ²⁻	0.02 ± 0.03	<dl–0.18	0.02 ± 0.02	<dl–0.05	0.04 ± 0.03	<dl–0.19
EC	0.4 ± 0.4	<dl–1.9	0.03 ± 0.1	<dl–0.5	0.4 ± 0.4	<dl–2.2
OC	1.8 ± 0.9	0.5–4.8	1.0 ± 0.5	0.4–3.3	2.8 ± 1.1	1.0–7.0
OC _{prim}	0.1 ± 0.1	<dl–0.7	n.a	n.a	0.1 ± 0.2	<dl–0.8
OC _{sec} ^a	1.6 ± 0.8	0.5–4.5	n.a	n.a	2.7 ± 1.0	0.9–6.6
WSOC	1.3 ± 0.8	0.1–4.0	n.a	n.a	n.a	n.a
WSOC/OC _{sec}	0.8 ± 0.2	0.2–1.1	n.a	n.a	n.a	n.a

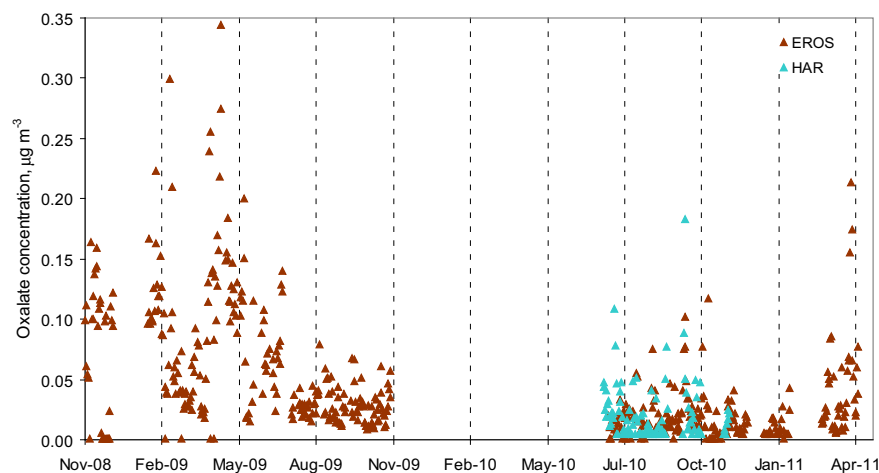
^a OC_{prim} and OC_{sec} calculated using an assumed OC_{prim}/EC ratio = 0.35.

partitioning of oxalic acid/oxalate do not give unequivocal predictions (Soonsin et al., 2010).

The mean oxalate concentration in the whole dataset had a very weak correlations with EC in PM_{2.5}, PM_{2.5–10} and PM₁₀ ($r = 0.07$, $r = -0.09$ and $r = 0.04$, respectively). This was anticipated from its regional distribution and reflects an insignificant contribution to oxalate from primary combustion sources. A similar observation was reported by Yao et al. (2004) and Yu et al. (2005), which clearly indicated little contribution of vehicular emissions to ambient oxalic acid. EC is strongly related to road traffic emissions at our site (Yin and Harrison, 2008; Yin et al., 2010). Moreover, a poor correlation between oxalate and potassium, a tracer for biomass burning, was observed in the fine fraction at EROS ($r = 0.18$) suggesting that primary biomass burning or rapid formation in biomass burning plumes was also not a major source of the oxalate. This is contrary to the measurements of Legrand et al. (2007) using data from K-Puszt (Hungary) and Aveiro (Portugal) who infer a major contribution of wood burning to oxalate concentrations in winter. In order to investigate secondary sources of oxalate aerosol,

the relationship between oxalate and secondary OC was determined and the plots of oxalate versus OC_{sec} in PM_{2.5} at EROS are shown in Fig. S2 (Supplemental Information). This figure shows that when all data ($n = 500$) are pooled, the two variables are weakly correlated ($r = 0.24$), but when sub-divided by season, show stronger correlations in spring ($r = 0.35$), and especially summer ($r = 0.55$). The high correlation coefficient found during summer suggests a photochemical and/or biogenic contribution to both secondary OC formation and to oxalate. This is in agreement with the results reported by Kawamura and Ikushima (1993) and Sempere and Kawamura (1994). The relatively low correlation between oxalate and SOC indicates that oxalate makes up a very variable proportion of secondary organic aerosol, but is typically 1–3% of SOA (after conversion of SOC to SOA mass), or 0.5–1.5% expressed as oxalate carbon/organic carbon.

Oxalate in coarse particles showed a modest correlation with nitrate and sulphate in summer ($r = 0.49$ and $r = 0.45$, respectively). Coarse oxalate may arise from gas-phase oxalic acid reacting with pre-existing particles, by particle coagulation or by heterogeneous

**Fig. 1.** Time series of oxalate concentrations in PM_{2.5} measured at EROS and Harwell sites.

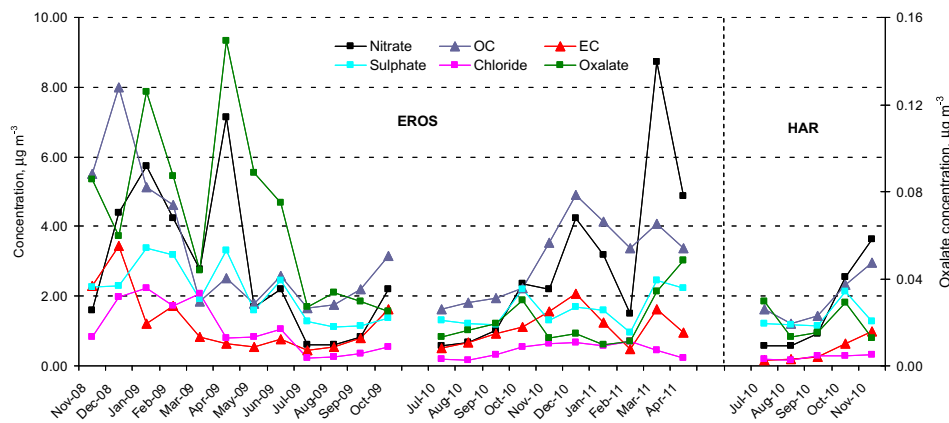


Fig. 2. Monthly average concentrations of major chemical components in PM_{2.5} at EROS and Harwell sites.

reactions within large droplets. However, for the full dataset, oxalate in the coarse mode correlated weakly with the other ionic species. The general assumption is that oxalate in ambient air is formed in the aqueous phase and therefore coarse mode oxalate can be produced by aqueous phase processes. Russell and Seinfeld (1998) have proposed that supermicron particles can be formed by in-cloud processes. Earlier studies by Dutton and Evans (1996) and Gadd (1999) have reported that oxalate was a by-product of the hydrolysis of oxaloacetate from citric acid and glyoxylate via the metabolic action of fungi in soil. Wind-blow soil might then be a source of oxalate in coarse airborne particles, but this seems unlikely to be a large contributor to airborne concentrations.

3.4. Size distribution of oxalate

The size distribution of oxalate was studied in comparison with major anionic and cationic species in ambient aerosol. Earlier studies have highlighted the strong similarities of the oxalate size distribution with that of sulphate (Kerminen et al., 2000; Huang et al., 2006).

In most of our samples, the mass size distributions of oxalate were bimodal consisting of one submicron mode and one supermicron mode. Some samples appeared to exhibit a more complex structure (Fig. 3). The dominant mode of oxalate peaked at 0.4 µm–0.5 µm with a more variable coarse mode around 1–2 µm. The finer mode was very similar to that of sulphate, seen in simultaneously collected material in Fig. S3 (Supplementary Information). This reflects the significant relationship between C₂O₄²⁻ and SO₄²⁻ in PM_{2.5} ($r = 0.60$) found at this site for the samples collected by Partisol Plus air samplers (500 samples). The similarity in size

distributions suggests that oxalate and sulphate may have similar formation pathways. Yao et al. (2002a) concluded that oxalate in the 0.32 µm–0.54 µm size range was produced by in-cloud processes and other studies have attributed sulphate in the droplet mode to in-cloud processes (Meng and Seinfeld, 1994; Kerminen and Wexler, 1995; Yu et al., 2005).

Oxalate has previously been attributed to a range of sources including primary emissions from vehicular transportation (Kawamura and Kaplan, 1987), biomass burning (Narukawa et al., 1999; Legrand et al., 2007), biogenic activity (Kawamura et al., 1996; Jones, 1998) and as a secondary product of the oxidation of both anthropogenic and biogenic precursors (Kalberer et al., 2001; Lim et al., 2005). Kawamura et al. (1996) and Kalberer et al. (2001) concluded that the condensation mode oxalate was from the photochemical formation in the gas phase by the reaction of organic compounds with photochemical oxidants such as OH free radicals and O₃ to form gaseous oxalic acid, followed by its condensation onto existing particles. If gas-particle condensation were the main process to form oxalate, the highest concentrations should be found in the condensation mode (0.175 µm–0.325 µm). On the contrary, the results showed the highest concentration of oxalate in the droplet mode, suggesting that condensation mode oxalate-containing particles were activated and became droplet mode particles due to cloud processing. A further proposed mechanism of formation of oxalic acid is from isoprene by in-cloud oxidation processes (Lim et al., 2005).

Oxalate in the coarse mode accounted for 12%–15% of total oxalate for the samples collected by cascade impactor. There were no significant correlations observed between cationic species and oxalate in the coarse mode. Similarities in coarse mode size distribution with sodium (1.8 µm–9.9 µm), suggest the possibility of formation within, or uptake of gaseous oxalate by sea salt particles. Alternatively, Russell and Seinfeld (1998) have proposed that supermicron particles can be formed by in-cloud processes.

3.5. Air mass trajectories

3.5.1. Full dataset at EROS

The 500 daily midday back trajectories arriving at EROS during the sampling period between November 2008 to April 2011 were generated by the HYSPLIT_4 model. The result of the cluster analysis of the 3-day trajectories is presented in Fig. 4. There were five main back trajectory clusters arriving at this site; cluster 1 – the fast south westerly accounted for 22% of the total trajectories, cluster 2 – the north westerly accounted for 21% of the total trajectories, cluster 3 – the slow southerly accounted for 19% of the total trajectories, cluster 4 – the fast westerly accounted for 9% of

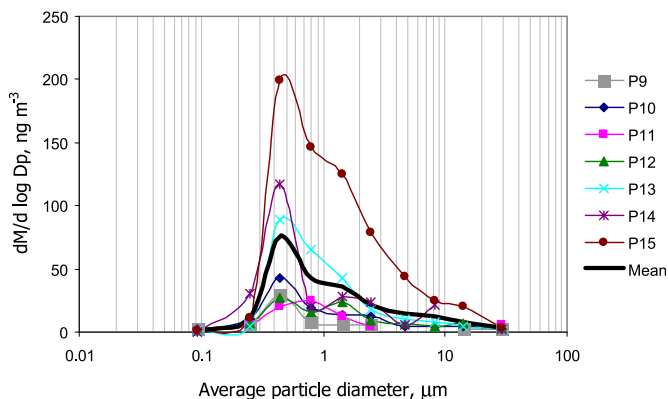


Fig. 3. Size distributions of oxalate in aerosol samples collected with by MOUDI impactor.

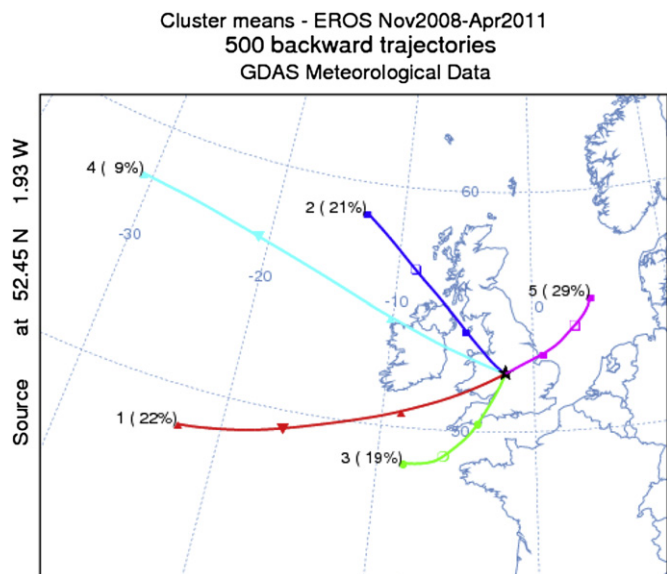


Fig. 4. Results of trajectory clustering for full EROS dataset.

the total trajectories, cluster 5 – the slow easterly accounted for 29% of the total trajectories. Cluster 5 occurred more frequently during autumn and spring. The fast maritime trajectory represented in cluster 4 occurred predominantly both in the winter and autumn months and less during the summer. Many of the trajectories during the summer grouped in the slow southerly airflow (cluster 3) whilst many of winter time trajectories appeared significantly both in cluster 2 and cluster 5. Table 4 contains the average concentration of oxalate and major components in the fine fraction for all trajectory clusters. The highest concentration of all species in PM except chloride are associated with the slow easterly (cluster 5) airflows. This result indicates that for the urban background site (EROS), the concentration of major secondary aerosol species would be expected to be associated with the long range transport of pollutants emitted from European mainland sources, consistent with the studies reported by Baker (2010), Abdalmogith and Harrison (2005) and Buchanan et al. (2002). As anticipated, the fast maritime cluster 4 originating from the Atlantic Ocean carries the highest chloride concentration of $1.12 \mu\text{g m}^{-3}$ Salvador et al. (2010) observed the source of oxalic and other diacids from central Europe, consistent with our trajectory observations.

A significant source of biogenic emissions from vegetation especially isoprene, could be a potential precursor associated with continental trajectories as stated by Legrand et al. (2007). Their study confirmed the role of isoprene as a precursor of oxalic acid associated with the high estimated isoprene emissions in Europe especially in the east flank of France (Simpson et al., 1995). This seems unlikely to be the main source, however, as this would produce a pronounced seasonality which is not observed.

Table 4

Average concentrations of major chemical components in $\text{PM}_{2.5}$ including mean temperature by trajectory clusters at EROS for the entire dataset.

$\text{PM}_{2.5}$	<i>n</i>	Concentration, $\mu\text{g m}^{-3}$								<i>T</i> (°C)
		SO_4^{2-}	NO_3^-	Cl^-	$\text{C}_2\text{O}_4^{2-}$	OC	EC	OC_{prim}	OC_{sec}	
Cluster 1	108	1.30	1.18	0.79	0.03	2.3	0.8	0.3	2.0	11
Cluster 2	105	1.59	2.04	0.69	0.04	3.3	1.3	0.4	2.8	9
Cluster 3	95	1.63	2.08	0.52	0.05	2.5	0.9	0.3	2.2	12
Cluster 4	45	1.49	1.40	1.12	0.05	2.6	0.9	0.3	2.3	8
Cluster 5	147	2.71	5.16	0.74	0.06	3.9	1.5	0.5	3.4	8

4. Conclusions

Previous work on atmospheric oxalate has highlighted both primary and secondary sources. The former have included both road traffic and biomass burning. However, in our dataset oxalate does not show a positive urban increment analogous to that of elemental carbon and does not correlate with EC and for this reason we discount road traffic as a significant source. The concentrations measured in our work, although comparable with many contemporary data (see Table 1) are generally lower than in older studies, suggesting that the road traffic source may have decreased with the advent of exhaust after-treatment devices. Additionally, we see no correlation between oxalate and fine potassium, a woodsmoke tracer, and we think it unlikely that biomass burning is contributing significantly to concentrations of oxalate.

A number of features of the behaviour of oxalate are consistent with a secondary, regional source. Mean concentrations are very similar at the urban and rural sites, and at the rural site oxalate is significantly correlated with the secondary inorganic components sulphate and nitrate. After clustering of air mass back trajectories, the highest concentrations of oxalate were found to be associated with air masses originating over the European mainland consistent with the behaviour of sulphate, nitrate and secondary organic carbon. It should, however, be noted that the elevation of oxalate in the continental trajectory is less than that for sulphate, nitrate or secondary organic carbon and the inter-site correlation between the urban EROS and rural Harwell sites is less strong for oxalate than for sulphate and nitrate. This is interpreted as oxalate having a number of secondary sources through different reaction pathways, depending upon different precursors which react at different rates, consequently leading to less spatial homogeneity than for sulphate and nitrate which have predominantly single precursor compounds. Biogenic precursors may play a role, but the lack of a substantial summer maximum suggests that this is not dominant.

The size distribution of oxalate sampled at the urban site bears strong similarities to that of sulphate suggesting common pathways in their formation either through aqueous phase formation processes or cloud processing subsequent to formation.

Appendix A. Supplementary data

Supplementary data related to this article can be found at <http://dx.doi.org/10.1016/j.atmosenv.2013.02.015>.

References

- Abdalmogith, S.S., Harrison, R.M., 2005. The use of trajectory cluster analysis to examine the long-range transport of secondary inorganic aerosol in the UK. *Atmospheric Environment* 39, 6686–6695.
- Arsene, C., Olariu, R.L., Zampas, P., Kanakidou, M., Mihalopoulos, N., 2011. Ion composition of coarse and fine particles in Iasi, north-eastern Romania: implications for aerosols chemistry in the area. *Atmospheric Environment* 45, 906–916.
- Baker, J., 2010. A cluster analysis of long range air transport pathways and associated pollutant concentrations within the UK. *Atmospheric Environment* 44, 563–571.
- Bao, L., Matsumoto, M., Kubota, T., Sekiguchi, K., Wang, Q., Sakamoto, K., 2012. Gas/particle partitioning of low-molecular-weight dicarboxylic acids at a suburban site in Saitama, Japan. *Atmospheric Environment* 47, 546–553.
- Buchanan, C.M., Beverland, I.J., Heal, M.R., 2002. The influence of weather-type and long-range transport on air particle concentration in Edinburgh, UK. *Atmospheric Environment* 36, 5343–5354.
- Castro, L.M., Pio, C.A., Harrison, R.M., Smith, D.J.T., 1999. Carbonaceous aerosol in urban and rural European atmospheres: estimation of secondary organic carbon concentrations. *Atmospheric Environment* 33, 2771–2781.
- Cavalli, F., Viana, M., Yttri, K.E., Genberg, J., Putaud, J.P., 2010. Toward a standardized thermal-optical protocol for measuring atmospheric organic and elemental carbon: the EUSAAR protocol. *Atmospheric Measurement Techniques* 3, 79–89.
- Cecinato, A., Amati, B., Palo, V.D., Marino, F., Possanzini, M., 1999. Determination of short-chain organic acids in airborne aerosols by ion chromatography. *Chromatographia* 50, 670–672.

- Chebbi, A., Carlier, P., 1996. Carboxylic acids in the troposphere, occurrence, sources, and sinks: a review. *Atmospheric Environment* 30, 4233–4249.
- Dabek-Zlotorzynska, E., McGrath, M., 2000. Determination of low-molecular-weight carboxylic acids in the ambient air and vehicle emission: a review. *Fresenius' Journal of Analytical Chemistry* 367, 507–518.
- Dutton, M.V., Evans, C.S., 1996. Oxalate production by fungi: its role in pathogenicity and ecology in the soil environment. *Canadian Journal of Microbiology* 42, 881–895.
- Falkovich, A.H., Graber, E.R., Schkolnik, G., Rudich, Y., Maenhaut, W., Artaxo, P., 2004. Low molecular weight organic acids in aerosol particles from Rondonia, Brazil, during the biomass-burning, transition and wet periods. *Atmospheric Chemistry and Physics*, 6867–6907. Discussions 4.
- Gadd, G.M., 1999. Fungal production of citric and oxalic acid: importance in metal speciation, physiology and biogeo-chemical processes. *Advances in Microbial Physiology* 41, 47–92.
- Harrison, R.M., Yin, J., 2008. Sources and processes affecting carbonaceous aerosol in central England. *Atmospheric Environment* 42, 1413–1423.
- Ho, K.F., Ho, S.S.H., Lee, S.C., Kawamura, K., Zou, S.C., Cao, J.J., Xu, H.M., 2011. Summer and winter variations of dicarboxylic acids, fatty acids and benzoic acid in PM_{2.5} in Pearl Delta River Region, China. *Atmospheric Chemistry and Physics* 11, 2197–2208.
- Huang, X.F., Yu, J.Z., He, L.Y., Yuan, Z., 2006. Water-soluble organic carbon and oxalate in aerosols at a coastal urban site in China: size distribution characteristics, sources, and formation mechanisms. *Journal of Geophysical Research* 111, D22212.
- Huang, Z., Harrison, R.M., Allen, A.G., James, J.D., Tilling, R.M., Yin, J., 2004. Field intercomparison of filter pack and impactor sampling for aerosol nitrate, ammonium, and sulphate at coastal and inland sites. *Atmospheric Research* 71, 215–232.
- Jacobson, M.C., Hansson, H.-C., Noone, K.J., Charlson, R.J., 2000. Organic atmosphere aerosols: review and state of the science. *Reviews of Geophysics* 38, 267–294.
- Jones, D.L., 1998. Organic acids in the rhizosphere – a critical review. *Plant Soil* 205, 25–44.
- Kalberer, M., Seinfeld, J.H., Yu, J.Z., Cocker, D.R., Morrical, B., Zenobi, R., 2001. Composition of SOA from cyclohexene oxidation and involved heterogeneous reactions. *Journal of Aerosol Science* 32, s907–s908.
- Karthikeyan, S., Balasubramanian, R., 2005. Rapid extraction of water soluble organic compounds from airborne particulate matter. *Analytical Sciences* 21, 1505–1508.
- Kawamura, K., Ikushima, K., 1993. Seasonal changes in the distribution of dicarboxylic acids in the urban atmosphere. *Environmental Science and Technology* 27, 2227–2235.
- Kawamura, K., Kaplan, I.R., 1987. Motor exhaust emissions as a primary source for dicarboxylic acids in Los Angeles ambient air. *Environmental Science and Technology* 21, 105–110.
- Kawamura, K., Usukura, K., 1993. Distributions of low molecular weight dicarboxylic acids in the North Pacific aerosol samples. *Journal of Oceanography* 49, 271–283.
- Kawamura, K., Kasukabe, H., Barrie, L.A., 1996. Source and reaction pathways of dicarboxylic acids, ketoacids and dicarbonyls in arctic aerosols: one year of observations. *Atmospheric Environment* 30, 1709–1722.
- Kerminen, V.M., Ojanen, C., Pakkanen, T., Hillamo, R., Aurela, M., Merilainen, J., 2000. Low-molecular-weight dicarboxylic acids in an urban and rural atmosphere. *Journal of Aerosol Science* 31, 349–362.
- Kerminen, V.M., Wexler, A.S., 1995. Growth laws for atmospheric aerosol particle: an examination of the bimodality of the accumulation mode. *Atmospheric Environment* 29, 3263–3275.
- Legrand, M., Preunkert, S., Oliveira, T., Pio, C.A., Hammer, S., Gelencser, A., Kasper-Giebl, A., Laj, P., 2007. Origin of C₂–C₅ dicarboxylic acids in the European atmosphere inferred from year-round aerosol study conducted at a west-east transect. *Journal of Geophysical Research* 112, D23S07.
- Lim, H.J., Carlton, A.G., Turpin, B.J., 2005. Isoprene forms secondary organic aerosol through cloud processing: model simulations. *Environmental Science and Technology* 39, 4441–4446.
- Limbeck, A., Kraxner, Y., Puxbaum, H., 2005. Gas to particle distribution of low molecular weight dicarboxylic acids at two different sites in central Europe (Austria). *Journal of Aerosol Science* 36, 991–1005.
- Limbeck, A., Puxbaum, H., Otter, L., Scholes, M.C., 2001. Semivolatile behavior of dicarboxylic acids and other polar organic species at a rural background site (Nylsvley, RSA). *Atmospheric Research* 35, 1853–1862.
- Meng, Z., Seinfeld, J.H., 1994. On the source of the submicrometer droplet mode of urban and regional aerosols. *Aerosol Science and Technology* 20, 253–265.
- Myriokefalitakis, S., Tsigaridis, K., Mihalopoulos, N., Sciare, J., Nenes, A., Kawamura, K., Segers, A., Kanakidou, M., 2011. In-cloud oxalate formation in the global troposphere: a 3-D modeling study. *Atmospheric Chemistry and Physics* 11, 5761–5782.
- Navukawa, M., Kawamura, K., Takeuchi, N., Nakajima, T., 1999. Distribution of dicarboxylic acids and carbon isotopic compositions in aerosols from 1997 Indonesian forest fires. *Geophysical Research Letters* 26, 3101–3104.
- Norton, R.B., Roberts, J.M., Huebert, B.J., 1983. Tropospheric oxalate. *Geophysical Research Letters* 10, 517–520.
- Pavuluri, C.M., Kawamura, K., Swaminathan, T., 2010. Water-soluble organic carbon, dicarboxylic acids, ketoacids, and α -dicarbonyls in the tropical Indian aerosols. *Journal of Geophysical Research* 115, D11302. <http://dx.doi.org/10.1029/2009JD012661>.
- Pio, C., Cerqueira, M., Harrison, R.M., Nunes, T., Mirante, F., Alves, C., Oliveira, C., Sanchez de la Campa, A., Artinano, B., Matos, M., 2011. OC/EC ratio observations in Europe: re-thinking the approach for apportionment between primary and secondary organic carbon. *Atmospheric Environment* 45, 6121–6132.
- Rohrl, A., Lammel, G., 2001. Low-molecular weight dicarboxylic acids and glyoxylic acids: seasonal and air mass characteristics. *Environmental Science and Technology* 35, 95–101.
- Russell, L.M., Seinfeld, J.H., 1998. Size and composition-resolved externally mixed aerosol model. *Aerosol Science and Technology* 28, 403–416.
- Saarnio, K., Aurela, M., Timonen, H., Saarikoski, S., Teinila, K., Makela, T., Sofiev, M., Koskinen, J., Aalto, P.P., Kulmala, M., Kukkonen, J., Hillamo, R., 2010. Chemical composition of fine particles in fresh smoke plumes from boreal wild-land fires in Europe. *Science of the Total Environment* 408, 2527–2542.
- Salvador, P., Artinano, B., Pio, C., Afonso, J., Legrand, M., Puxbaum, H., Hammer, S., 2010. Evaluation of aerosol sources at European high altitude background sites with trajectory statistical methods. *Atmospheric Environment* 44, 2316–2329.
- Sempere, R., Kawamura, K., 1994. Comparative distribution of dicarboxylic acids and related polar compounds in snow, rain, and aerosols from urban atmosphere. *Atmospheric Environment* 28, 449–459.
- Sempere, R., Kawamura, K., 1996. Low molecular weight dicarboxylic acids and related polar compounds in the remote marine rain samples collected from western Pacific. *Atmospheric Environment* 30, 1609–1619.
- Simpson, D., Guenther, A., Hewitt, C.N., Steinbrecher, R., 1995. Biogenic emissions in Europe. *Journal of Geophysical Research* 100 (D11), 22,875–22,890.
- Soonsin, V., Zardini, A.A., Marcolli, C., Züend, A., Krieger, K., 2010. The vapor pressures and activities of dicarboxylic acids reconsidered: the impact of the physical state of the aerosol. *Atmospheric Chemistry & Physics* 10, 11753–11767.
- Stohl, A., 1998. Computation, accuracy and applications of trajectories – a review and bibliography. *Atmospheric Environment* 32, 947–966.
- Sunset Laboratory Inc, 2004. A Guide to Running and Maintaining the Sunset Laboratory OCEC Analyser. February 2.
- Wang, Y., Zhuang, G., Chen, S., An, Z., Zhen, A., 2007. Characteristics and sources of formic, acetic and oxalic acids in PM_{2.5} and PM₁₀ aerosols in Beijing, China. *Atmospheric Research* 84, 169–181.
- Yao, X., Fang, M., Chan, C.K., 2002a. Size distribution and formation of dicarboxylic acid in atmospheric particles. *Atmospheric Environment* 36, 2099–2107.
- Yao, X., Chan, C.K., Fang, M., Cadle, S., Chan, T., Mulawa, P., He, K., Ye, B., 2002b. The water-soluble ionic composition of PM_{2.5} in Shanghai and Beijing, China. *Atmospheric Environment* 36, 4223–4234.
- Yao, X., Lau, A.P.S., Fang, M., Chan, C.K., Hu, M., 2003. Size distributions and formation of ionic species in atmospheric particulate pollutants in Beijing, China: 2-dicarboxylic acids. *Atmospheric Environment* 37, 3001–3007.
- Yao, X., Fang, M., Chan, C.K., Ho, K.F., Lee, S.C., 2004. Characterization of dicarboxylic acids in PM_{2.5} in Hong Kong. *Atmospheric Environment* 38, 963–970.
- Yin, J., Harrison, R.M., 2008. Pragmatic mass closure study for PM₁₀, PM_{2.5} and PM₁₀ at roadside, urban background and rural sites. *Atmospheric Environment* 42, 980–988.
- Yin, J., Harrison, R.M., Chen, Q., Rutter, A., Schauer, J.J., 2010. Source apportionment of fine particles at urban background and rural sites in the UK atmosphere. *Atmospheric Environment* 44, 841–851.
- Yu, J.Z., Huang, X.F., Xu, J., Hu, M., 2005. When aerosol sulfate goes up, so does oxalate: implication for the formation mechanisms of oxalate. *Environmental Science and Technology* 39, 128–133.
- Zhang, Q., Jimenez, J.L., Canagaratna, M.R., Allan, J.D., Coe, H., Ulbrich, I., Alfarra, M.R., Takami, A., Middlebrook, A.M., Sun, Y.L., Dzepina, K., Dunlea, E., Docherty, K., DeCarlo, P.F., Salcedo, D., Onasch, T., Jayne, J.T., Miyoshi, T., Shimojo, A., Hatakeyama, S., Takegawa, N., Kondo, Y., Schneider, J., Drewnick, F., Borrmann, S., Weimer, S., Demerjian, K., Williams, P., Bower, K., Bahreini, R., Cottrell, L., Griffin, R.J., Rautiainen, J., Sun, J.Y., Zhang, Y.M., Worsnop, D.R., 2007. Ubiquity and dominance of oxygenated species in organic aerosols in anthropogenically-influenced Northern Hemisphere midlatitudes. *Geophysical Research Letters* 34, L13801.